Article type : Original Article

OsHKT1;5 mediates Na^+ exclusion in the vasculature to protect leaf blades and reproductive tissues from salt toxicity in rice

Natsuko I. Kobayashi[1], Naoki Yamaji[2], Hiroki Yamamoto[3], Kaoru Okubo[3], Hiroki Ueno[4], Alex Costa[5,8], Keitaro Tanoi[1,9], Hideo Matsumura[4], Miho Fujii-Kashino[2], Tomoki Horiuchi[3], Mohammad Al Nayef[6], Sergey Shabala[6], Gynheung An[7], Jian Feng Ma[2], Tomoaki Horie[3]

[1] Graduate School of Agricultural and Life Sciences, The University of Tokyo, 1-1-1, Yayoi, Bunkyo-ku, Tokyo 113–8657, Japan

[2] Institute of Plant Science and Resources, Okayama University, Chuo 2-20-1, Kurashiki, Japan

[3] Division of Applied Biology, Faculty of Textile Science and Technology, Shinshu University, 3-15-1, Tokida, Ueda, Nagano 386-8567, Japan

[4] Gene Research Center, Shinshu University, 3-15-1, Tokida, Ueda, Nagano 386-8567, Japan

This article has been accepted for publication and undergone full peer review but has not been through the copyediting, typesetting, pagination and proofreading process, which may lead to differences between this version and the Version of Record. Please cite this article as doi: 10.1111/tpj.13595

[5] Department of Biosciences, University of Milan, Via G. Celoria 26, 20133 Milan, Italy

[6] School of Agricultural Science, University of Tasmania, Private Bag 54, Hobart, Tas 7001, Australia

[7] Crop Biotech Institute, Kyung Hee University, Youngin, Kyungbuk 446-701, Republic of Korea

[8] Institute of Biophysics, Consiglio, Nazionale delle Ricerche, Via G. Celoria 26, 20133 Milan, Italy

[9] PRESTO, Japan Science and Technology Agency (JST), 4-1-8 Honcho, Kawaguchi, Saitama 332-0012, Japan

For correspondence:

Tomoaki Horie

Division of Applied Biology, Faculty of Textile Science and Technology,

Shinshu University, 3-15-1, Tokida, Ueda, Nagano 386-8567, Japan

Phone: +81-268-21-5561

Fax: +81-268-21-5561

email: horie@shinshu-u.ac.jp

email address: Natsuko I. Kobayashi (anikoba@g.ecc.u-tokyo.ac.jp); Naoki Yamaji (n-yamaji@rib.okayama-u.ac.jp); Hiroki Yamamoto (m.16141514.m@gmail.com); Kaoru Okubo (k.okubo.186@gmail.com); Hiroki Ueno (bisulphite@gmail.com); Alex Costa (alex.costa@unimi.it); Keitaro Tanoi (uktanoi@g.ecc.u-tokyo.ac.jp); Hideo Matsumura (hideoma@shinshu-u.ac.jp); Miho Fujii-Kashino (m-fujii@rib.okayama-u.ac.jp); Tomoki Horiuchi (6fs720h@shinshu-u.ac.jp); Mohammad Al Nayef (mohammad.alnayef@utas.edu.au); Sergey Shabala (sergey.shabala@utas.edu.au); Gynheung An (genean@khu.ac.kr); Jian Feng Ma (maj@rib.okayama-u.ac.jp); Tomoaki Horie (horie@shinshu-u.ac.jp)

Running title: OsHKT1;5-mediated Na^+ exclusion in rice

Key words: salt tolerance, Na^+ exclusion, HKT, xylem, phloem, *Oryza sativa*

Footnote: Present address of H.U., Institute of Vegetable and Floriculture Science, NARO, 360 Kusawa, Anno, Tsu, Mie 23 514-2392, Japan.

SUMMARY

Salt tolerance QTL analysis of rice has revealed that the *SKC1* locus, which is involved in a higher K^+/Na^+ ratio in shoots, corresponds to the *OsHKT1;5* gene encoding a Na^+-selective transporter. However, physiological roles of OsHKT1;5 in rice exposed to salt stress remain elusive and no *OsHKT1;5* gene disruption mutants have been characterized to date. In this study, we dissected two independent T-DNA insertional *OsHKT1;5* mutants. Measurements of ion contents in tissues and $^{22}Na^+$ tracer imaging experiments showed that loss-of-function of OsHKT1;5 in salt-stressed rice roots triggers massive Na^+ accumulation in shoots. Salt stress-induced increases in the *OsHKT1;5* transcript was observed in roots and basal stems including basal nodes. Immuno-staining using an anti-OsHKT1;5 peptide antibody indicated that OsHKT1;5 is localized in cells adjacent to the xylem in roots. Additionally, direct introduction of $^{22}Na^+$ tracer to leaf sheaths also demonstrated the involvement of OsHKT1;5 in xylem Na^+ unloading in leaf sheaths. Furthermore, OsHKT1;5 was indicated to present in the plasma membrane and found to localize also in the phloem of diffuse vascular bundles in basal nodes. Together with the characteristic $^{22}Na^+$ allocation in the blade of the developing immature leaf in the mutants, these results suggest a novel function of OsHKT1;5 in mediating Na^+ exclusion in the phloem to prevent Na^+ transfer to young leaf blades. Our findings further demonstrate that the function of OsHKT1;5 is crucial over growth stages of rice, including the protection of the next generation seeds as well as of vital leaf blades under salt stress.

INTRODUCTION

Soil salinization is a severe environmental stress, which limits the productivity of agricultural crops. Salinization can commonly occur due to agricultural practices associated with irrigation and nearly 50% of irrigated lands in the world, which is approximately 230 Mha, is estimated to be salt-affected (Pitman and Läuchli, 2002, Ruan *et al.*, 2010, Shabala, 2013, Suzuki *et al.*, 2016). Not only irrigation but seawater incursions into rivers and aquifers in coastal areas can be a serious source of salinization (Pitman and Läuchli, 2002). Soil salinization occurs frequently in arid and semi-arid regions, however, it is also widespread in humid regions such as South and Southeast Asia (Szabolcs and Pessarakli, 2010), where rice cultivation is primal as staple food production. Over-accumulation of salts outside of roots and inside of the plant body leads to two major problems, water deficit and ion toxicity (Munns and Tester, 2008, Horie *et al.*, 2012, Deinlein *et al.*, 2014).

Na^+ is one of the major toxic elements in salt-affected soil. A significant attention has been paid to the function of the high-affinity K^+ transporter (HKT) family because of the robust permeability for Na^+ when this cation exists in excess (Schachtman and Schroeder, 1994, Rubio *et al.*, 1995, Rubio *et al.*, 1999). Analyses of the structure and the transport property of HKTs led to the notion that HKT transporters can be classified into at least two subfamilies, class I and class II (Mäser *et al.*, 2002b, Horie *et al.*, 2009). In contrast to the class II subfamily that in general shows Na^+-K^+ co-transport activity, class I HKT transporters exhibits

Na^+-selective transport with poor K^+ permeability (Horie *et al.*, 2009). AtHKT1;1, a class I transporter in *Arabidopsis thaliana*, was demonstrated to function in Na^+ transport (Uozumi *et al.*, 2000) and Na^+ exclusion from leaves during salt stress by mediating Na^+ unloading from the xylem particularly in roots (Mäser *et al.*, 2002a, Sunarpi *et al.*, 2005, Davenport *et al.*, 2007, Møller *et al.*, 2009).

In rice, the *OsHKT1;5* gene has been narrowed down as a salt tolerance determinant by the quantitative trait loci (QTL) analysis (Ren *et al.*, 2005). The locus from a tolerant variety was originally targeted as the QTL that leads to higher K^+ accumulation in shoots during salt stress and therefore designated as the *shoot K^+ content 1* (*SKC1*). The *Saltol* locus is one of the major salt tolerance QTL of rice, which is involved in Na^+/K^+ homeostasis during salt stress (Thomson *et al.*, 2010), and the *SKC1* locus was later found to be localized within the *Saltol* locus (Ismail and Horie, 2017). The *OsHKT1;5* gene, the product of which showed preferred Na^+ selective transport in heterologously-expressed cells, was demonstrated to have rather a larger influence on the reduction of Na^+ concentration in shoots (Ren *et al.*, 2005). In addition, the salt tolerance QTL analysis using durum wheat (*T. turgidum*) has revealed that the *TmHKT1;5-A* gene derived from a wild wheat relative *T. monococcum* corresponds to the *Na^+ exclusion 2* (*Nax2*) QTL that contributes to lowering of the Na^+ level in leaves (James *et al.*, 2006, Byrt *et al.*, 2007). Phenotypic analyses on the near isogenic line for *Nax2* under salt stress indicated that the *Nax2* locus governs superior Na^+ exclusion from leaf blades facilitating

more K^+ accumulation by mediating Na^+ unloading from the xylem in roots (James *et al.*, 2006, Byrt *et al.*, 2007). In fact, the near isogenic line (NIL) of durum wheat harboring *TmHKT1;5-A* increased grain yield by 25% compared to NILs without the locus in salt-affected fields (Munns *et al.*, 2012). Furthermore, studies strongly suggested that *TaHKT1;5-D* is the causal gene for the *Kna1* locus which has long been known to achieve efficient leaf Na^+ exclusion maintaining a higher K^+/Na^+ ratio in leaves in bread wheat that shows higher tolerance to salt stress compared with durum wheat (Gorham *et al.*, 1987, Gorham *et al.*, 1990, Byrt *et al.*, 2014). However, in the above studies in rice and wheat, no gene disruption alleles in *HKT1;5* genes have been reported or investigated to date.

HKT1;5-dependent leaf Na^+ exclusion systems in rice and wheat are considered to be analogous to the mechanism mediated by AtHKT1;1 in Arabidopsis (Horie *et al.*, 2009). However, the Na^+ exclusion mechanism in such crops appear to be more complicated as, unlike the case of *AtHKT1;1*, multiple *HKT* genes exist in those species (Garciadeblás *et al.*, 2003, Huang *et al.*, 2008). Indeed, another important allele for Na^+ exclusion, *Nax1*, was identified in parallel with *Nax2* by wheat QTL analysis (Lindsay *et al.*, 2004, James *et al.*, 2006). The *Nax1* was later predicted to be the *TmHKT1;4-A2* gene from *T. monococcum*, which also encodes a class I transporter (Huang *et al.*, 2006). The *Nax1* locus contributes to Na^+ exclusion from leaf blades by mediating Na^+ unloading not only in roots but also in leaf sheaths under salt stress (James *et al.*, 2006). However, another study using the same *Nax* lines have suggested that *Nax*

loci confer two highly complementary mechanisms, both of which contribute towards reducing the xylem Na^+ content. One enhances the retrieval of Na^+ back into the root stele via HKT1;4 or HKT1;5, whilst the other reduces the rate of Na^+ loading into the xylem via SOS1 (Zhu *et al.*, 2016). Thus, the actual role of HKT1 in Na^+ unloading from the xylem may be not as straightforward as above experiments have suggested. Evidence has accumulated that class I transporters in rice, OsHKT1;1 and OsHKT1;4, are also involved in the mechanism of Na^+ exclusion from leaf blades during salt stress (Cotsaftis *et al.*, 2012, Takagi *et al.*, 2015, Wang *et al.*, 2015, Suzuki *et al.*, 2016).

Based on these findings, the involvement of OsHKT1;5 in the Na^+ exclusion from leaves is predicted, however, detailed physiological roles of OsHKT1;5 remain to be elucidated. In this study, we have characterized two independent T-DNA mutants of rice for the *OsHKT1;5* gene, and carried out physiological experiments including $^{22}Na^+$ tracer studies. This study provides evidence that OsHKT1;5-dependent Na^+ transport in roots, leaf sheaths, and stems is a key salt tolerance mechanism over growth stages of rice. Presented results also provide insight into a new physiological function of OsHKT1;5 under salt stress.

RESULTS

Subcellular localization of OsHKT1;5 in leaf sheath protoplasts of rice

Either the enhanced green fluorescent protein (EGFP) or a chimeric OsHKT1;5 fused with EGFP at the N-terminal (EGFP-OsHKT1;5) were transiently co-expressed with a plasma membrane (PM) marker orange fluorescent protein (OFP)-fused to CBL1n (Held *et al.*, 2011) in protoplasts from leaf sheaths of rice seedlings. In confocal microscopy, green fluorescence of EGFP-OsHKT1;5-expressing cells was observed in the periphery of the cells and overlapped well with the red fluorescence from CBL1n-OFP (Figure 1a-d). In contrast, green fluorescence was broadly detected inside of control cells expressing EGFP alone and no overlap with the red fluorescence was observed (Figure 1e-h). These results indicate that OsHKT1;5 is targeted to the PM in rice cells.

Isolation of *OsHKT1;5* mutants

Homozygous mutants (HM) and their sibling WT (WT) plants were isolated from two independent T-DNA mutant lines of rice for *OsHKT1;5*, 3D-00458 and 4A-02764 (Figure 2a). No mature *OsHKT1;5* transcript was detected in 00458-HM plants by RT-PCR using 10-day-old whole rice seedlings (Figure 2b). On the other hand, 02764-HM plants showed a reduction in the *OsHKT1;5* transcript in comparison with the level of WT plants (Figure 2b).

These results suggested that the 00458-HM plant is a knockout mutant, while the 02764-HM plant might be a mutant that shows abnormal expression of *OsHKT1;5*.

Accumulation and distribution of Na^+ in the *OsHKT1;5* null mutant under salt stress

To investigate the influence of dysfunction of *OsHKT1;5* under salt stress, the *OsHKT1;5* null mutant was characterized at first. Na^+ concentration in different tissues was measured using 3 to 4-week-old plants treated with 50 mM NaCl for 3 days. 00458-HM plants accumulated more Na^+ in leaf blades and sheaths but less Na^+ in basal stems in comparison with WT (Figure 3a). $^{22}Na^+$ tracer experiments were carried out to further dissect OsHKT1;5-mediated Na^+ transport. Distribution image of $^{22}Na^+$ radiation and increased shoot/root and blade/sheath $^{22}Na^+$ ratios indicated that 00458-HM plants rapidly draw $^{22}Na^+$ into shoots and eventually into leaf blades (Figure 3b, c, d). The line profiling using the L3 sheath showed a gradual increase in the amount of $^{22}Na^+$ in the 00458-HM mutant as the location gets closer to the junction between the blade and sheath compared with WT plants, supporting above-mentioned results (Figure 3e). An additional experiment using a compartment box showed that vigorous $^{22}Na^+$ accumulation in the root of 00458-WT plants was lost in 00458-HM plants when $^{22}Na^+$ was added to a part of the root (Figure S1).

Tissue specificity of *OsHKT1;5* gene expression and its product

To have a better insight into the role of OsHKT1;5-mediated Na^+ transport in rice, immuno-staining using an anti-OsHKT1;5 peptide antibody was conducted. 3 to 4-week-old of 00458-HM and -WT plants were treated with 50 mM NaCl for 3 days. Immuno-staining on tissue sections of WT plants resulted in detecting strong immuno-signals within the vascular regions of the crown root and the basal node (Figure 4a, c, e). In the root, signals were predominantly detected in cells next to the protoxylem and the metaxylem I (Figure 4c). In the basal node, interestingly, strong signals were identified in the phloem of some diffuse vascular bundles (DVBs) (Figure 4e, g, i). The 00458-HM mutant revealed no reliable signal in the same experiment conducted in parallel, supporting the fidelity of OsHKT1;5-derived immuno-signals in WT plants (Figure 4b, d, f, h).

In tissues of different developmental stages, the *OsHKT1;5* transcript was found to be robust in roots throughout the stages (Figure 5a). Notably, a substantial increase in the *OsHKT1;5* transcript level was detected in tissues composing the stem and ear structures such as nodes, internodes, peduncles and rachises with the highest expression in node I (Figure 5a). Furthermore, a laser microdissection (LMD)-mediated quantitative real time PCR (qPCR) analysis revealed the predominant expression of *OsHKT1;5* in diffuse vascular bundles (DVBs) with a reduced level of expression in enlarged vascular bundles (EBVs), which was comparable level to that in the basal stem (Figure 5b).

The function of OsHKT1;5 in the reproductive growth stage of rice under salt stress

Given the fact that *OsHKT1;5* expression level was highly increased in the stem during the reproductive growth stage (Figure 5), 00458-HM and -WT plants, which were about to start heading, were treated with a long-term salt stress. A gradual increase in the NaCl concentration from 25 mM to 100 mM for more than 1 month led to more severe damage to the null mutant in visual with a trend of withering of old leaves compared with WT plants (Figure 6a). Measurements of the Na^+ content in upper tissues have indicated that 00458-HM plants accumulate significantly higher Na^+ in flag leaves and peduncles but not in nodes and lower internodes (Figure 6b). On the other hand, the K^+ content was decreased in flag leaves and nodes (Figure 6c). The weight of seeds of the null mutant exhibited an approximately 11 % reduction compared to WT plants (Figure 6d). Furthermore, seeds from the null mutant showed a lower germination rate than that of WT (Figure 6e).

The mutant line 02764 is a unique material: *OsHKT1;5* expression profile in the mutant

We performed qPCR analysis on *OsHKT1;5* expression in 02764-HM plants considering that the T-DNA inserted in the promoter region harbors an enhancer element constituted of the CaMV 35S core promoter (Jeong *et al.*, 2002). In roots of approximately 3-week-old 02764-WT plants, salt stress significantly increased the level of *OsHKT1;5* transcripts,

however, insertion of a T-DNA largely diminished its transcript level in the 02764-HM mutant irrespective of salt stress (Figure 7a). In shoots of 02764-HM plants grown under the control condition, the *OsHKT1;5* transcript level was significantly increased in blades and sheaths of young leaves but not in basal stems in comparison with 02764-WT plants (Figure 7b). Under salt stress, the transcript level in leaves of both 02764-WT and -HM plants was maintained or even decreased compared with control (Figure 7b). Note however that, in the basal stem, increases in the *OsHKT1;5* transcript by salt in WT roots was impaired in the mutant (Figure 7b). Results of immuno-staining using the line 02764 showed that expression of OsHKT1;5 was severely reduced in roots and basal nodes of the 02764-HM mutant in comparison with the sibling WT (Figure S2). However, no apparent immuno-signal was detected in leaf sheaths of both WT and mutant even though *OsHKT1;5* expression is significantly higher in the mutant (Figure 7b), for which the reason is not clear. These results indicated that the 02764-HM mutant is not a simple gene knockdown line but overexpresses *OsHKT1;5* in leaf sheaths and blades with severe reductions in its expression in roots and salt-induced up-regulation in basal stems.

Accumulation and distribution of Na^+ in the 02764-HM mutant and their impact on the growth under salt stress

Patterns of Na^+ accumulation and Na^+ distribution in tissues were also investigated using the line 02764. 02764-HM plants showed the trait of Na^+ over-accumulation in leaves (Figure 8a). However, Na^+ accumulation was prominent in leaf sheaths but not in blades that rather exhibited less Na^+ accumulation in this stress condition in contrast to the pattern of Na^+ accumulation in leaves of the 00458-HM mutant (Figures 3a, 8a). Na^+ over-accumulation in young leaf sheaths of 02764-HM plants was also observed under more severe salt stress, accompanied with trends with a slight increase in Na^+ accumulation in leaf blades and basal stems as well (Figure S3). $^{22}Na^+$ tracer analysis further revealed that the 02764-HM mutant draw more $^{22}Na^+$ into shoots compared with WT plants (Figure 8b, c). However, the blade/sheath ratio and the line profiling of the youngest expanding leaf (L3) again indicated that a considerable amount of $^{22}Na^+$ was retained in the sheath region of 02764-HM plants compared with WT plants (Figure 8d, e). These results suggested that 02764-HM plants overexpressing *OsHKT1;5* in sheaths block the Na^+ transfer to leaf blades more efficiently than WT plants.

Growth of 02764-HM plants was monitored to evaluate the influence of unusual *OsHKT1;5* expression and Na^+ distribution. Approximately 2-week-old hydroponically grown plants were treated with 0, 40 or 80 mM NaCl for 21 days. The growth and biomass of the

02764-HM line showed a growth reduction of 25% and 72%, at 40 and 80 mM of NaCl, respectively, compared to the control (Figure 9a, b). Whereas WT plants showed only a slight growth reduction of 5% at 40 mM, and 25% at 80 mM of NaCl (Figure 9a, b). The mutant exhibited significant decreases in the number of tillers per plant ($p < 0.01$) in contrast to WT (Figure 9c).

Distinctive allocation of $^{22}Na^{+}$ in two independent *OsHKT1;5* mutants

The role of OsHKT1;5 in leaf sheaths was further evaluated by direct $^{22}Na^{+}$ introduction to the sheath of 4-week-old rice plants after cutting the roots out. The line profiling analysis on the sheath of the leaf 6 (L6) revealed robust Na^{+} retention of 02764-HM plans similar to WT plants in a sharp contrast to that of 00458-HM plants (Figure 10a). Blade/sheath Na^{+} ratios of young leaves, L6 and L7, were significantly higher in 00458-HM plants than those of 02764-HM and WT plants (Figure 10b). These results indicate that OsHKT1;5 is involved in transport of Na^{+} via xylem in the leaf sheath.

We also investigated Na^{+} distribution by $^{22}Na^{+}$ tracer experiments to quantitatively evaluate the amount of Na^{+} that reaches to young leaves including the newest developing leaf. Na^{+} accumulation in young expanded leaves, L7 and L8, of approximately 4-week-old plants exposed to a mild salt stress showed similar trends to the previous observation such that

00458-HM plants allow Na^+ over-accumulation in leaf blades, while the level of Na^+ in blades of 02764-HM and WT plants is low (Figures 10c). Note, however, that the newest immature leaf (L9) that yet hides in the sheath of L8 and remains as a sink tissue exhibited a similar level of Na^+ over-accumulation in both mutants (Figure 10c).

DISCUSSION

OsHKT1;5-mediated Na^+ unloading from the xylem in rice suffering salt stress

Phenotypic evaluation of the two *OsHKT1;5* mutant alleles demonstrated that dysfunction of OsHKT1;5 in roots leads to substantial Na^+ over-accumulation in leaves of both homozygous mutants in the vegetative growth stage in response to salt stress (Figures 2, 3, 8). Immunostaining analyses using the anti-OsHKT1;5 peptide antibody on *OsHKT1;5* mutants and their sibling WT revealed that OsHKT1;5 preferentially localizes in cells next to the protoxylem and the metaxylem I in rice roots (Figures 4a-d, S2a-d). Together with the result of the plasma membrane localization of OsHKT1;5 in rice cells (Figure 1), these data provide compelling evidence that OsHKT1;5 prevents Na^+ transfer from roots to shoots in the presence of a large amount of Na^+, most likely by mediating Na^+ unloading from the xylem as has been expected (Horie *et al.*, 2009, Hauser and Horie, 2010). Note that the term "Na^+ unloading from

the xylem" signifies a process, in which transporters located at the xylem parenchyma cell interface retrieve Na^+ from apoplastic space, which results in reducing diffusive transfer of Na^+ into the xylem vessel that is a dead tissue. A working model of OsHKT1;5 in roots in response to salt stress is shown in Figure 11.

The 02764-HM mutant was found to exhibit a distinct profile of *OsHKT1;5* gene expression such that the mutant overexpresses the *OsHKT1;5* gene in leaves with a severe reduction in its expression in roots (Figure 7a, b), presumably due to the location of the T-DNA insertion (Figure 2) and the enhancer trap element that the T-DNA encompasses (Jeong *et al.*, 2002). Overexpression of *OsHKT1;5* in leaf sheaths, however, shed light on the role of OsHKT1;5 in sheaths of rice under salt stress. Measurements of Na^+ contents in tissues and $^{22}Na^+$-imaging analyses revealed that OsHKT1;5 prevents Na^+ transfer to young leaf blades in sheaths (Figures 8a, d, e, 10). Direct introduction of $^{22}Na^+$-containing solution to leaf sheaths strongly suggested that OsHKT1;5-mediated Na^+ exclusion in leaf sheaths predominantly occurs via Na^+ unloading from the xylem (Figure 10a, b). In wheat, the *TmHKT1;5-A* gene homoeologous to *OsHKT1;5* was reported to function in Na^+ unloading from the xylem predominantly in roots, but Na^+ exclusion at the xylem of leaf sheaths was indicated to be mediated by the *TmHKT1;4-A2* gene (James et al., 2006; Huang et al., 2006; Byrt et al., 2007). In contrast, the contribution of OsHKT1;4 to Na^+ exclusion from leaf blades appears to be minor in rice affected by salt stress during the vegetative growth stage, even though *OsHKT1;4*

expresses in leaf sheaths (Suzuki *et al.*, 2016). Taken together, the above-mentioned results demonstrate that OsHKT1;5 mediates Na^+ unloading from the xylem in roots and leaf sheaths to avoid Na^+ over-accumulation in young leaf blades upon salt stress (Figure 11).

Given that *OsHKT1;5* overexpression in leaf sheaths resulted in better Na^+ exclusion from blades (Figures 8, 10), it was intriguing that *OsHKT1;5* transcript levels in sheaths of japonica rice cultivars tended to be decreased in response to salt stress (Figures 7b, S4). Investigation into the relation among *OsHKT1;5* expression in leaf sheaths, Na^+ concentrations in leaf blades, and overall salt tolerance across broad rice accessions might be an interesting subject to pursue.

OsHKT1;5-mediated Na^+ transport in the phloem: a novel physiological role of OsHKT1;5

$^{22}Na^+$ tracer experiments indicated that both 00458-HM and 02764-HM mutants over-accumulated Na^+ in the newest leaf (L9) having no structural discrimination between the blade and the sheath, in contrast to the pattern of Na^+ accumulation in leaf blades of youngest-expanded leaves (L7 and L8) of the two mutants (Figure 10c). This result implies that the leaf protection mechanism by OsHKT1;5 from salt stress might not be simply dependent only on Na^+ unloading from the xylem.

In support of this notion, immuno-staining indicated robust expression of OsHKT1;5 in the phloem of some diffuse vascular bundles (DVBs) of basal nodes (Figures 4e-i; S2e-h), which are connected to younger leaves (Hoshikawa, 1989). As shown in Figure 7b, a salt-inducible increase in the *OsHKT1;5* transcript in basal stems was abolished in the 02764-HM mutant. The lack of *OsHKT1;5* induction might cause deficiency in the activity of OsHKT1;5-dependent Na^+ transport, necessary for dealing with increased Na^+ ions in this tissue under salt stress. Consistently, an immune-staining analysis on the line 02764 revealed that immuno-signals in DVBs of basal nodes of the homozygous mutant were severely reduced under salt stress in comparison with the sibling WT (Figure S2e-h). Based on these results, we assume that OsHKT1;5 also mediates Na^+ exclusion in phloem parenchyma cells in the DVB of basal nodes in order to prevent Na^+ transfer to phloem sieve tubes that function in upward sap flow, through which Na^+ can be translocated to young leaf blades (Figure 11).

Impact of OsHKT1;5-mediated Na^+ transport on salt tolerance of rice

Two independent T-DNA insertional mutations in the *OsHKT1;5* gene gave rise to no growth penalty under any of control conditions tested or in short-term salt stress conditions. qPCR analyses revealed that *OsHKT1;5* gene expression characteristically increases in tissues that constitute the stem and the panicle in the reproductive growth stage (Figure 5a). Long-term salt

stress on 00458-HM plants in the reproductive growth stage resulted in slight but apparent damage in visual, especially in old leaves in comparison with 00458-WT plants (Figure 6a). The largest influence was found in the Na^+ content of flag leaf blades that are a key tissue supplying assimilation products to panicles, indicating a high impact of OsHKT1;5 function on the protection of the vital blades from salt stress at this stage as well (Figure 6b). The disruption of *OsHKT1;5* also had a minor influence on the K^+ accumulation in flag leaf blades and nodes, which suggest that the relevance of OsHKT1;5-mediated Na^+ exclusion to the K^+ homeostasis may be indirect (Figure 6c). On the other hand, however, it is noteworthy that the dysfunction of OsHKT1;5 caused a significant reduction in the K^+ content in flag leaf blades (Figure 6b, c) because it indicates that OsHKT1;5-mediated Na^+ transport achieves a higher K^+/Na^+ content ratio in vital leaf blades, known to be an essential parameter for plant salt tolerance (Hauser and Horie, 2010, James *et al.*, 2011).

The *OsHKT1;5* transcript level in node I, which is the uppermost node connected to the peduncle and the flag leaf, was found to be robust (Figure 5a). As has been recently well described by Yamaji and Ma (2014), nodes play a key role in the distribution of mineral elements including toxic elements, which are translocated from the root. Different types of vascular bundles exist in nodes, including enlarged vascular bundles (EVBs) and diffuse vascular bundles (DVBs). In the case of node I, EVBs and DVBs were connected to the flag leaf and the panicle, respectively (Yamaji and Ma, 2014). *OsHKT1;5* transcripts were detected

in both EVBs and DVBs of node I with a much higher degree of accumulation in DVBs (Figure 5b), which suggests a large impact on the Na^+ homeostasis of the panicle and seeds under salt stress. Indeed, the lack of OsHKT1;5 resulted in an approximately 11% reduction in the weight of 1000 seeds compared with WT under salt stress (Figure 6d). Moreover, lower germination rates of seeds harvested from the null mutant indicated a negative impact of loss-of-function of OsHKT1;5 on the quality of seeds (Figure 6e).

A long-term salt stress on the mature 02764-HM mutant also resulted in causing more damage to the mutant than WT (Figures 9). Even though the distinct overexpression of *OsHKT1;5* in leaf sheaths prevented Na^+ over-accumulation in blades in short-term salt stress conditions, prolonged stress treatments with higher concentrations of NaCl can be presumed to exceed the capacity for blocking the Na^+ transfer to blades (Figures 8, 10a, b, S3), suggesting a major importance of OsHKT1;5-mediated Na^+ transport activity in roots for a reduction in Na^+ toxicity during salt stress.

Evidence has accumulated that *OsHKT1;1* and *OsHKT1;4* genes, orthologues of *OsHKT1;5* in rice, also contribute to Na^+ exclusion from leaf blades in rice exposed to salt stress (Cotsaftis *et al.*, 2012, Takagi *et al.*, 2015, Wang *et al.*, 2015, Suzuki *et al.*, 2016), which suggest potential functional redundancy among the three *OsHKT1* genes in the Na^+ exclusion

mechanism in rice. Nevertheless, *OsHKT1;5* mutants used in this study showed the remarkable disturbance in Na^+ homeostasis and visual damage due to salt stress, providing evidence of the essentiality of OsHKT1;5 on the overall salt tolerance of rice over the investigated growth stages. Allele mining of the *HKT1;5* gene using accessions from *O. sativa* and *O. glaberrima* has revealed that seven major alleles of *HKT1;5* identified are strongly associated with leaf Na^+ concentrations across diverse accessions (Platten *et al.*, 2013). Moreover, among the seven alleles, the japonica allele was expected to confer the lowest Na^+ exclusion from leaves under salt stress (Platten *et al.*, 2013). It is thus intriguing to investigate whether specific differences in the sequence of the alleles make a direct influence on leaf Na^+ concentrations, and if so, whether any causal sequence can be determined among them in addition to key nucleotide substitutions between a salt tolerant landrace Nona Bokra and a sensitive japonica cv. Koshihikari, reported by Ren et al., (2005).

METHODS AND MATERIALS

Plant materials and growth conditions

Japonica rice cultivars Dongjin and Nipponbare (*Oryza sativa* L.) were used in this study. Possible independent T-DNA mutants for *OsHKT1;5* were found at the Rice Functional Genomic Express Database (http://signal.salk.edu/cgi-bin/RiceGE). Homozygous mutants that

harbor a T-DNA insertion in the *OsHKT1;5* gene were isolated from the lines PFG-TDA_3D-00458 and PFG-TDA_4A-02764 using the specific primers (see Table S1). At the same time, sibling WT to each mutant was isolated from the same parent line as the homozygous mutants.

Seeds were surface sterilized and germinated as described previously (Horie *et al.*, 2001). For the preparation of rice plants in the vegetative growth stage, hydroponic culture was performed using a growth chamber with a light/dark cycle of 16/8 h at 28-30 °C. Kimura B nutrient solution was in general used (Ma *et al.*, 2001) except for the test of the salt sensitivity of PFG-TDA_4A-02764, for which the growth medium was Hoagland solution: 1.25 mM KNO_3; 0.5 mM $Ca(NO_3)_2$, 0.5 mM $MgSO_4$; 42.5 µM Fe-EDTA; 0.625 mM KH_2PO_4; 0.16µM $CuSO_4$; 0.38 µM $ZnSO_4$; 1.8 µM $MnSO_4$; 45 µM H_3BO_3; 0.015 µM $(NH_4)_2MO_7O_{24}$; 0.01 µM $CoCl_2$ (pH 5.5–6.0). Saline hydroponic solution containing the indicated amount of NaCl was applied for salt stress.

Approximately 10-day-old rice seedlings from the line PFG-TDA_3D-00458 were transferred to plastic pots filled with the paddy-field soil and grown in a greenhouse. The homozygous mutant and WT plants were planted side by side in the same pot. Salt stress was initiated with 25 mM NaCl-containing tap water just before soil-grown plants started heading, and the concentration was gradually increased by 25 mM up to 100 mM for more than a month (Suzuki *et al.*, 2016). For the measurement of ion contents, two independent plants per

genotype from two different pots were used and six randomly-selected stems were sampled in each pot. As for yield estimation and the test for the seed germination rate, seeds were harvested from three independent plants per genotype, planted in three different pots.

Subcellular localization analysis using rice protoplasts

For the fusion of the enhanced GFP (EGFP) at the N-terminal of OsHKT1;5, the *OsHKT1;5* cDNA was amplified by PCR using specific primers containing *Xba*I (5') and *Bam*HI (3') restriction sites. For the primers, see Table S1. Amplified fragments were subcloned downstream of EGFP in frame in pBI221 (Horie *et al.*, 2007).

Protoplasts were isolated from leaf sheath of 7-day-old rice seedlings and transformed as described previously (Zhang *et al.*, 2011, Suzuki *et al.*, 2016). In brief, a PM marker CBL1n-OFP (Held *et al.*, 2011) was mixed with either EGFP-OsHKT1;5 or free EGFP and added to isolated protoplasts. Then polyethylene glycol (PEG 4000) solution was added. The protoplasts were re-suspended in the WI solution (0.5 M mannitol, 20 mM KCl, 4 mM MES, pH 5.7) and kept in the dark at 24 °C. Confocal microscope and image analyses were performed as described in Suzuki et al. (2016).

Total RNA extraction and RT-PCR analyses

Total RNA was extracted from rice tissues using an RNeasy Plant Mini Kit (Qiagen, Limburg, Netherlands). Reverse transcription and the real-time PCR (qPCR) analysis were performed as described previously (Yamaji *et al.*, 2013, Suzuki *et al.*, 2016). Primers used for RT-PCR analyses were listed in Table S1.

To analyze the tissue specific expression of *OsHKT1;5* in node I, qPCR analysis was performed using the same samples, which were derived from vascular bundles of node I and used for the analysis on *OsHKT1;4* expression (Suzuki *et al.*, 2016).

Measurements of ion contents

Measurements of ion concentration in rice tissues were performed as described previously (Suzuki *et al.*, 2016). In brief, tissue samples were harvested and washed with ultrapure water twice and dried at 65 °C. Then all samples were digested using ultrapure nitric acid (Kanto Chemical, Japan) for 1-2 days and boiled at 95 °C for 10 min three times. Ion contents were determined using an inductively coupled plasma optical emission spectrometer (ICP-OES; SPS3100, SII Nano Technology Inc., Japan).

Immuno-histological staining of OsHKT1;5

The synthetic peptide TATTHDEVELGLGRRNKRGC (positions 167–186 of OsHKT1;5) was produced by immunizing rabbits to obtain the peptide antibody against OsHKT1;5. Tissues including basal nodes and roots at the vegetative stage (approximately 3-4 weeks old plants) of *OsHKT1;5* mutants and their sibling WTs, treated with 50 mM NaCl for 3 days, were used for immunostaining of the OsHKT1;5 protein as described previously (Yamaji and Ma, 2007, Yamaji *et al.*, 2013). Fluorescence of secondary antibody (Alexa Fluor 555 goat anti-rabbit IgG, Molecular Probes) was observed using a confocal laser-scanning microscopy (LSM700; Carl Zeiss).

$^{22}Na^{+}$ imaging analysis

To trace the Na^{+} transport, plants were treated with the nutrient solution containing 10 mM NaCl and $^{22}Na^{+}$ (4.4 kBq/ml), and then the roots were washed with the ice-cooled nutrient solution for 10 min. The $^{22}Na^{+}$ absorption period was 30 min for 2-week-old seedlings, 3 hours for 4-week-old seedlings. The radiation of $^{22}Na^{+}$ in each tissue was analyzed using either the NaI counter (ARC-300, Aloka) to calculate the amount of Na^{+} (nmol) or quantitatively visualized using an imaging-plate (IP) (BAS IP MS, GE Healthcare Lifescience) and a FLA-5000 image analyzer (FUJIFILM Co., Ltd.) with the resolution of 100 μm. The

distribution of $^{22}Na^{+}$ in leaf tissues was recorded by setting the region of interest (ROI), and their sum was presented as the amount of $^{22}Na^{+}$ in the shoot. Consequently, the shoot/root ratio and the blade/sheath ratio were determined as the ratio between the amount of $^{22}Na^{+}$ in each specified tissue. The line profile data of $^{22}Na^{+}$ along sheath samples was obtained by setting the long narrow ROI as described previously (Suzuki *et al.*, 2016).

For the direct introduction of $^{22}Na^{+}$ into the xylem of leaf sheaths, the shoot part of 4-week-old plants was cut at the position of 5 mm above the root, and the cut-surface was soaked in the solution contained 15 mM KCl, 1 mM $MgSO_4$, 1 mM $Ca(NO_3)_2$, 0.5 mM NaH_2PO_4, and 1.8 kBq/ml $^{22}NaCl$ for 30 min. The image of $^{22}Na^{+}$ distribution in each leaf part was obtained using an IP.

The multi-compartment transport box experiment using 1-week-old seedlings was performed as described previously (Kobayashi *et al.*, 2013). $^{22}Na^{+}$ (2 kBq/ml) was applied in the nutrient solution only in the middle compartment where the root region of 1-2 cm from the root tip was placed. $^{22}Na^{+}$ (2 kBq/ml) was applied for 15 min to the root region of 1-2 cm from the root tip, and the allocation of $^{22}Na^{+}$ was quantitatively visualized (Figure S1).

ACKNOWLEDGEMENTS

This work was supported by the Ministry of Education, Culture, Sports, Science and Technology (MEXT) of Japan (25119709 to T.H.), MEXT as part of the Joint Research Program implemented at the Institute of Plant Science and Resources, Okayama University in Japan (2615, 2716 to T.H.), and the Public Foundation of Chubu Science and Technology Center (to T.H.). This work was also supported by the Japan Science and Technology Agency (JST) [PRESTO] (# 15665950) to K. T., Ministero dell'Istruzione, dell'Università e della Ricerca through the FIRB 2010 program (RBFR10S1LJ_001) and by the Linea 2 Project from the University of Milan to A.C., and the Australian Research Council grant to S.S. We would like to thank Prof. Julian I. Schroeder (UC San Diego) for his critical reading of the manuscript. Some initial research of T.H. was supported by a National Institutes of Environmental Health Sciences grant (P42 ES010337) to Prof. Schroeder.

The authors declare no conflict of interest.

SHORT LEGENDS FOR SUPPORTING INFORMATION

Figure S1: $^{22}Na^{+}$ tracer analysis on a knockout mutant for *OsHKT1;5* using a compartment box

Figure S2: Immuno-staining of the second mutant line (02764) for *OsHKT1;5*.

Figure S3: Na^+ contents in upper tissues of 02764-HM and -WT plants in response to 75 mM and 100 mM NaCl

Figure S4: *OsHKT1;5* expression in a japonica rice cultivar Nipponbare treated with or without 50 mM NaCl

Table S1: The list of primers used in this study

REFERENCES

Byrt, C.S., Platten, J.D., Spielmeyer, W., James, R.A., Lagudah, E.S., Dennis, E.S., Tester, M. and Munns, R. (2007) HKT1;5-like cation transporters linked to Na^+ exclusion loci in wheat, *Nax2* and *Kna1*. *Plant Physiol.*, **143**, 1918-1928.

Byrt, C.S., Xu, B., Krishnan, M., Lightfoot, D.J., Athman, A., Jacobs, A.K., Watson-Haigh, N.S., Plett, D., Munns, R., Tester, M. and Gilliham, M. (2014) The Na^+ transporter, TaHKT1;5-D, limits shoot Na^+ accumulation in bread wheat. *Plant J.*, **80**, 516-526.

Cotsaftis, O., Plett, D., Shirley, N., Tester, M. and Hrmova, M. (2012) A two-staged model of Na^+ exclusion in rice explained by 3D modeling of HKT transporters and alternative splicing. *PLoS ONE.*, **7**, e39865.

Davenport, R.J., Munoz-Mayor, A., Jha, D., Essah, P.A., Rus, A. and Tester, M. (2007) The Na^+ transporter AtHKT1;1 controls retrieval of Na^+ from the xylem in *Arabidopsis*. *Plant Cell Environ.*, **30**, 497-507.

Deinlein, U., Stephan, A.B., Horie, T., Luo, W., Xu, G. and Schroeder, J.I. (2014) Plant salt-tolerance mechanisms. *Trends in Plant Sci.*, **19**, 371-379.

Garciadeblás, B., Senn, M., Banuelos, M. and Rodriguez-Navarro, A. (2003) Sodium transport and HKT transporters: the rice model. *Plant J.*, **34**, 788-801.

Gorham, J., Hardy, C., Wyn Jones, R.G., Joppa, L.R. and Law, C.N. (1987) Chromosomal location of a K/Na discriminating character in the D genome of wheat. *Theor. Appl. Genet.*, **74**, 584-588.

Gorham, J., Wyn Jones, R.G. and Bristol, A. (1990) Partial characterization of the trait for enhanced K^+-Na^+ discrimination in the D genome of wheat. *Planta.*, **180**, 590-597.

Hauser, F. and Horie, T. (2010) A conserved primary salt tolerance mechanism mediated by HKT transporters: a mechanism for sodium exclusion and maintenance of high K/Na ratio in leaves during salinity stress. *Plant Cell Environ.*, **33**, 552-565.

Held, K., Pascaud, F., Eckert, C., Gajdanowicz, P., Hashimoto, K., Corratge-Faillie, C., Offenborn, J.N., Lacombe, B., Dreyer, I., Thibaud, J.B. and Kudla, J. (2011) Calcium-dependent modulation and plasma membrane targeting of the AKT2 potassium channel by the CBL4/CIPK6 calcium sensor/protein kinase complex. *Cell Res.*, **21**, 1116-1130.

Horie, T., Costa, A., Kim, T.H., Han, M.J., Horie, R., Leung, H.Y., Miyao, A., Hirochika, H., An, G. and Schroeder, J.I. (2007) Rice OsHKT2;1 transporter mediates large Na^+ influx component into K^+-starved roots for growth. *EMBO J.*, **26**, 3003-3014.

Horie, T., Hauser, F. and Schroeder, J.I. (2009) HKT transporter-mediated salinity resistance mechanisms in *Arabidopsis* and monocot crop plants. *Trends Plant Sci.*, **14**, 660-668.

Horie, T., Karahara, I. and Katsuhara, M. (2012) Salinity tolerance mechanisms in glycophytes: An overview with the central focus on rice plants. *Rice*, **5**.

Horie, T., Yoshida, K., Nakayama, H., Yamada, K., Oiki, S. and Shinmyo, A. (2001) Two types of HKT transporters with different properties of Na^+ and K^+ transport in *Oryza sativa*. *Plant J.*, **27**, 129-138.

Hoshikawa, K. (1989) The growing rice plants. *Nosan Gyoson Bunka Kyokai (Nobunkyo), Akasaka, Minato-ku, Tokyo 107, Japan*.

Huang, S., Spielmeyer, W., Lagudah, E.S., James, R.A., Platten, J.D., Dennis, E.S. and Munns, R. (2006) A sodium transporter (HKT7) is a candidate for *Nax1*, a gene for salt tolerance in durum wheat. *Plant Physiol.*, **142**, 1718-1727.

Huang, S., Spielmeyer, W., Lagudah, E.S. and Munns, R. (2008) Comparative mapping of *HKT* genes in wheat, barley, and rice, key determinants of Na^+ transport, and salt tolerance. *J Exp Bot.*, **59**, 927-937.

Ismail, A.M. and Horie, T. (2017) Genomics, Physiology, and Molecular Breeding Approaches for Improving Salt Tolerance. *Annu Rev Plant Biol* (in press)., doi: 10.1146/annurev-arplant-042916-040936.

James, R.A., Blake, C., Byrt, C.S. and Munns, R. (2011) Major genes for Na^+ exclusion, *Nax1* and *Nax2* (wheat *HKT1;4* and *HKT1;5*), decrease Na^+ accumulation in bread wheat leaves under saline and waterlogged conditions. *J Exp Bot.*, **62**, 2939-2947.

James, R.A., Davenport, R.J. and Munns, R. (2006) Physiological characterization of two genes for Na^+ exclusion in durum wheat, *Nax1* and *Nax2*. *Plant Physiol.*, **142**, 1537-1547.

Jeong, D.H., An, S., Kang, H.G., Moon, S., Han, J.J., Park, S., Lee, H.S., An, K. and An, G. (2002) T-DNA insertional mutagenesis for activation tagging in rice. *Plant Physiol.*, **130**, 1636-1644.

Kobayashi, N.I., Iwata, N., Saito, T., Suzuki, H., Iwata, R., Tanoi, K. and Nakanishi, T.M. (2013) Different magnesium uptake and transport activity along the rice root axis revealed by ^{28}Mg tracer experiments. *Soil Sci Plant Nutr.*, **59**, 149-155.

Lindsay, M.P., Lagudah, E.S., Hare, R.A. and Munns, R. (2004) A locus for sodium exclusion *Nax1*, a trait for salt tolerance, mapped in durum wheat *Funct. Plant Biol.*, **31**, 1105-1114.

Møller, I.S., Gilliham, M., Jha, D., Mayo, G.M., Roy, S.J., Coates, J.C., Haseloff, J. and Tester, M. (2009) Shoot Na^+ exclusion and increased salinity tolerance engineered by cell type-specific alteration of Na^+ transport in Arabidopsis. *The Plant Cell*, **21**, 2163-2178.

Mäser, P., Eckelman, B., Vaidyanathan, R., Horie, T., Fairbairn, D.J., Kubo, M., Yamagami, K., Yamaguchi, K., Nishimura, M., Uozumi, N., Robertson, W., M.R., S. and Schroeder, J.I. (2002a) Altered shoot/root Na^+ distribution and bifurcating salt sensitivity in *Arabidopsis* by genetic disruption of the Na^+ transporter AtHKT1. *FEBS Lett.*, **531**, 157-161.

Mäser, P., Hosoo, Y., Goshima, S., Horie, T., Eckelman, B., Yamada, K., Yoshida, K., Bakker, E.P., Shinmyo, A., Oiki, S., Schroeder, J.I. and Uozumi, N. (2002b) Glycine residues in potassium channel-like selectivity filters determine potassium selectivity in four-loop-per-subunit HKT transporters from plants. *Proc. Natl. Acad. Sci. U.S.A.*, **99**, 6428-6433.

Ma, J.F., Goto, S., Tamai, K. and Ichii, M. (2001) Role of root hairs and lateral roots in silicon uptake by rice. *Plant physiology*, **127**, 1773-1780.

Munns, R., James, R.A., Xu, B., Athman, A., Conn, S.J., Jordans, C., Byrt, C.S., Hare, R.A., Tyerman, S.D., Tester, M., Plett, D. and Gilliham, M. (2012) Wheat grain yield on saline soils is improved by an ancestral Na^+ transporter gene. *Nat Biotech.*, **30**, 360-364.

Munns, R. and Tester, M. (2008) Mechanisms of salinity tolerance. *Ann Rev Plant Biol.*, **59**, 651-681.

Pitman, M.G. and Läuchli, A. (2002) Global Impact of Salinity and Agricultural Ecosystems. In: Salinity: Environment-Plants -Molecules (Läuchli, A., Lüttge, U., eds). *Dordrecht, the Netherlands: Kluwer*, Chapter 1, 3-20.

Platten, J.D., Egdane, J.A. and Ismail, A.M. (2013) Salinity tolerance, Na^+ exclusion and allele mining of *HKT1;5* in *Oryza sativa* and *O. glaberrima*: many sources, many genes, one mechanism? *BMC Plant Biol.*, **13**, 32.

Ren, Z.H., Gao, J.P., Li, L.G., Cai, X.L., Huang, W., Chao, D.Y., Zhu, M.Z., Wang, Z.Y., Luan, S. and Lin, H.X. (2005) A rice quantitative trait locus for salt tolerance encodes a sodium transporter. *Nat. Genet.*, **37**, 1141-1146.

Ruan, C.J., da Silva, J.A.T., Mopper, S., Qin, P. and Lutts, S. (2010) Halophyte improvement for a salinized world. *Crit Rev Plant Sci.*, **29**, 329-359.

Rubio, F., Gassmann, W. and Schroeder, J.I. (1995) Sodium-driven potassium uptake by the plant potassium transporter HKT1 and mutations conferring salt tolerance. *Science*, **270**, 1660-1663.

Rubio, F., Schwarz, M., Gassmann, W. and Schroeder, J.I. (1999) Genetic selection of mutations in the high affinity K^+ transporter HKT1 that define functions of a loop site for reduced Na^+ permeability and increased Na^+ tolerance. *J Biol Chem.*, **274**, 6839-6847.

Sasaki, A., Yamaji, N., Mitani-Ueno, N., Kashino, M. and Ma, J.F. (2015) A node-localized transporter OsZIP3 is responsible for the preferential distribution of Zn to developing tissues in rice. *Plant J.*, **84**, 374-384.

Schachtman, D.P. and Schroeder, J.I. (1994) Structure and transport mechanism of a high-affinity potassium uptake transporter from higher plants. *Nature*, **370**, 655-658.

Shabala, S. (2013) Learning from halophytes: physiological basis and strategies to improve abiotic stress tolerance in crops. *Ann Bot.*, **112**, 1209-1221.

Sunarpi, Horie, T., Motoda, J., Kubo, M., Yang, H., Yoda, K., Horie, R., Chan, W.Y., Leung, H.Y., Hattori, K., Konomi, M., Osumi, M., Yamagami, M., Schroeder, J.I. and Uozumi, N. (2005) Enhanced salt tolerance mediated by AtHKT1 transporter-induced Na^+ unloading from xylem vessels to xylem parenchyma cells. *Plant J.*, **44**, 928-938.

Suzuki, K., Yamaji, N., Costa, A., Okuma, E., Kobayashi, N.I., Kashiwagi, T., Katsuhara, M., Wang, C., Tanoi, K., Murata, Y., Schroeder, J.I., Ma, J.F. and Horie, T. (2016) OsHKT1;4-mediated Na^+ transport in stems contributes to Na^+ exclusion from leaf blades of rice at the reproductive growth stage upon salt stress. *BMC Plant Biol.*, **16**, 22.

Szabolcs, I. and Pessarakli, M. (2010) Soil salinity and sodicity as particular plant/crop stress factors. *Handbook of Plant and Crop Stress, Third Edition (CRC Press)*, 3-21.

Takagi, H., Tamiru, M., Abe, A., Yoshida, K., Uemura, A., Yaegashi, H., Obara, T., Oikawa, K., Utsushi, H., Kanzaki, E., Mitsuoka, C., Natsume, S., Kosugi, S., Kanzaki, H., Matsumura, H., Urasaki, N., Kamoun, S. and Terauchi, R. (2015) MutMap accelerates breeding of a salt-tolerant rice cultivar. *Nat Biotech.*

Thomson, M.J., Ocampo, M., Egdane, J., Rahman, M.A., Sajise, A.G., Adorada, D.L., Tumimbang-Raiz, E., Blumwald, E., Seraj, J.I., Singh, R.K., Gregorio, G.B. and Ismail, A.M. (2010) Characterizing the *Saltol* quantitative trait locus for salinity tolerance in rice. *Rice*, **3**, 148-160.

Uozumi, N., Kim, E.J., Rubio, F., Yamaguchi, T., Muto, S., Tsubota, A., Bakker, E.P., Nakamura, T. and Schroeder, J.I. (2000) The *Arabidopsis HKT1* gene homologue mediates inward Na^+ currents in *Xenopus* oocytes and Na^+ uptake in *Saccharomyces cerevisiae*. *Plant Physiol.*, **121**, 1249-1259.

Wang, R., Jing, W., Xiao, L., Jin, Y., Shen, L. and Zhang, W. (2015) The Rice High-Affinity Potassium Transporter1;1 Is Involved in Salt Tolerance and Regulated by an MYB-Type Transcription Factor. *Plant Physiol.*, **168**, 1076-1090.

Yamaji, N. and Ma, J.F. (2007) Spatial distribution and temporal variation of the rice silicon transporter Lsi1. *Plant Physiol.*, **143**, 1306-1313.

Yamaji, N. and Ma, J.F. (2014) The node, a hub for mineral nutrient distribution in graminaceous plants. *Trends in Plant Sci.*, **19**, 556-563.

Yamaji, N., Sasaki, A., Xia, J.X., Yokosho, K. and Ma, J.F. (2013) A node-based switch for preferential distribution of manganese in rice. *Nat Commun.*, **4**, 2442.

Zhang, Y., Su, J., Duan, S., Ao, Y., Dai, J., Liu, J., Wang, P., Li, Y., Liu, B., Feng, D., Wang, J. and Wang, H. (2011) A highly efficient rice green tissue protoplast system for transient gene expression and studying light/chloroplast-related processes. *Plant Methods.*, **7**, 30.

Zhu, M., Shabala, L., Cuin, T.A., Huang, X., Zhou, M., Munns, R. and Shabala, S. (2016) *Nax* loci affect SOS1-like Na^+/H^+ exchanger expression and activity in wheat. *J Exp Bot.*, **67**, 835-844.

FIGURE LEGENDS

Figure 1. Subcellular localization of EGFP-OsHKT1;5, transiently expressed in rice protoplasts under the control of the 35S promoter. (a) EGFP-derived green fluorescence from a single focal plane of a typical rice protoplast from leaf sheaths. The plasma membrane marker CBL1n-OFP was co-expressed with EGFP-OsHKT1;5 in the same protoplasts. (b) OFP-derived red fluorescence from the same protoplast shown in a. (c) A merged image of a and b. (d) Bright filed image of the protoplast shown in a to c. (e) EGFP-derived green fluorescence from a single focal plane of a typical rice protoplast from leaf sheaths. CBL1n-OFP was co-expressed with EGFP in the same protoplasts. (f) OFP-derived red fluorescence from the same protoplast shown in e. (g) A merged image of e and f. (h) A bright field image of the protoplast shown in e to g. Note that experiments were repeated several times with eight independent protoplasts preparation in total and we routinely detected the signal in the plasma membrane.

Figure 2. Isolation of two independent mutants of japonica rice (cv. Dongjin) harboring a T-DNA insertion in the *OsHKT1;5* gene. (a) A schematic diagram of the two mutant alleles: 3D-00458 and 4A-02764, and the result of RT-PCR. Pale grey boxes and a dark grey box represent exons and the promoter region of *OsHKT1;5*, respectively. Black and white

arrowheads indicate the T-DNA insertion site in each mutant line and primers used for RT–PCR, respectively. (b) Results of RT-PCR using 10-day-old whole rice seedlings: homozygous mutants, sibling WT of each mutant, and Dongjin.

Figure 3. Profiles of accumulation and distribution of Na^+ in the *OsHKT1;5* knockout mutant under salt stress. (a) Na^+ contents in each tissue of 00458-HM (black bars) and 00458-WT (white bars) plants. 3-week-old rice plants were prepared by hydroponic culture and treated with 50 mM NaCl for 3 days. L6B, 6th leaf blade; L5B, 5th leaf blade; L6S, 6th leaf sheath; L5S, 5th leaf sheath; BS, basal stem; R, root. (b) Allocation of $^{22}Na^+$ in shoots of rice plants after 30 min of the uptake of the tracer in roots. A picture of shoots from 2-week-old rice plants and the image of $^{22}Na^+$ radiation captured by the imaging plate (IP) were shown. 3 independent plants from each line are presented. Shoots were separated into leaf 1 to 4. As for the leaf 3 (L3), it was further separated into the blade and the sheath. (c) Distribution ratio of $^{22}Na^+$ between the shoot and the root in each rice line (n=3, ±SD). (d) Distribution ratio of $^{22}Na^+$ between the blade and the sheath of L3 in each rice line (n=3, ±SD). (e) $^{22}Na^+$ line profiles along the sheath of L3 of each line based on the IP data shown in b. Results of 2 independent plants per each line are shown in triangles and circles: Red, cv. Dongjin; blue, 00458-HM; green, 00458-WT. The Student's-t test was performed vs. WT (a) and Dongjin (c, d), respectively: * $P < 0.05$, ** $P < 0.01$.

Figure 4. Immuno-staining of the OsHKT1;5 protein using an anti-OsHKT1;5 peptide antibody. 3 to 4-week-old of 00458-HM and -WT plants, exposed to 50 mM NaCl, were used. Immuno-signals are shown in red. (a) Cross-section of a crown root of WT. (b) Cross-section of a crown root of the mutant. (c) Enlarged image of the vascular region of the root of WT, surrounded by the white square in a. ED, endodermis layer; MXI, mataxylem I; MXII, metaxylem II; PX, protoxylem; PP, protophloem. (d) Enlarged image of the vascular region of the root of the mutant, surrounded by the white square in b. (e) Cross section of the basal stem of WT. (f) Cross section of the basal stem of the mutant. (g) Enlarged image of a diffuse vascular bundle (DVB) region of the basal node of WT, surrounded by the white square in e. (h) Enlarged image of a DVB region of the basal node of the mutant, surrounded by the white square in f. (i) Enlarged image of the DVB of WT, surrounded by the yellow square in g. Note that the blue color in all panels corresponds to cell wall ultraviolet auto-fluorescence.

Figure 5. Growth stage-dependent and tissue specific expression profiles of *OsHKT1;5* in a japonica rice cultivar Nipponbare. Results of qPCR for *OsHKT1;5* are shown. (a) RNA samples were prepared from rice plants at indicated growth stages as described previously (Yamaji et al., 2013) (n=3, ±SD). Expression of *OsHKT1;5*, relative to the root of 14-week-old plants, is shown. (b) Expression of *OsHKT1;5* in vasculatures of node I and the basal stem is shown. RNA samples were prepared from enlarged vascular bundles (EBVs) and diffuse

vascular bundles (DVBs) of node I using the LMD (Sasaki *et al.*, 2015, Suzuki *et al.*, 2016) as well as the basal stem (BS). Relative *OsHKT1;5* expression in each part is shown setting its expression in the EVB to 1 (n = 5-8, ±SD).

Figure 6. Impacts of a null mutation in *OsHKT1;5* on phenotypes of the mutant in the reproductive growth stage under salt stress. 00458-HM and -WT plants were grown in the same pot filled with paddy-filed soil. Approximately 3-month-old plants were exposed to salt stress by gradually increasing the concentration of NaCl in the tap water from 25 mM to 100 mM for more than a month. (a) Typical visual phenotype of the 00458-HM mutant after the salt treatment. (b, c) Na^+ and K^+ contents in tissues of the stem and the flag leaf of 00458-WT (white bars) and 00458-HM (black bars) plants (n=12, ±SD). (d) Estimated weights of 1000 seeds harvested from 00458-WT and -HM plants after the salt treatment. Harvested seeds from 3 independent pots were mixed and the weight of 100 seeds selected at random was measured 4 times, based on which the weight of 1000 seeds was estimated (±SD). (e) Germination rates of the seeds. 100 seeds selected at random from above-mentioned seed populations were germinated on a 1 mM $CaSO_4$ solution. The same test was repeated 4 times (±SD). The Student's-t test was used for the statistical analysis: * $P < 0.05$ (HM vs. WT).

Figure 7. qPCR analyses on *OsHKT1;5* in tissues of the 02764-HM mutant and its sibling WT. (a) Results of qPCR for *OsHKT1;5* using 3-week-old 02764-HM and 02764-WT plants. Expression of *OsHKT1;5* in roots, relative to roots in the control condition, is shown (n=6, ±SD). An asterisk (*) indicates a significant difference ($P < 0.05$, the Student's-t test: WT vs. HM). (b) Results of qPCR using tissues in shoots. Expression of *OsHKT1;5* in young leaves and basal stems, relative to the 6th leaf blade in the control condition, is shown (n=6, ±SD). L6B, 6th leaf blades; L6S, 6th leaf sheaths; L5B, 5th leaf blades; L5S, 5th leaf sheaths; BS, basal stem. Different alphabets represent significant differences at the level of 5% (the Tukey's test).

Figure 8. Profiles of accumulation and distribution of Na^+ in the 02764-HM mutant under salt stress. (a) Na^+ contents in each tissue of 02764-HM (grey bars) and 02764-WT (white bars) plants. 3-week-old rice plants were prepared by hydroponic culture and treated with 50 mM NaCl for 3 days. L6B, 6th leaf blade; L5B, 5th leaf blade; L6S, 6th leaf sheath; L5S, 5th leaf sheath; BS, basal stem; R, root. (b) Allocation of $^{22}Na^+$ in shoots of rice plants after 30 min of the uptake of the tracer in roots. A picture of shoots from 2-week-old rice plants and the image of $^{22}Na^+$ radiation captured by an imaging plate (IP). 3 independent plants from each line are shown. Shoots were separated into leaf 1 to 4. As for the leaf 3 (L3), it was further separated into the blade and the sheath. (c) Distribution ratio of $^{22}Na^+$ between the shoot and the root in

each rice line (n=3, ±SD). (d) Distribution ratio of $^{22}Na^{+}$ between the blade and the sheath of L3 in each rice line (n=3, ±SD). (e) $^{22}Na^{+}$ line profiles along the sheath of L3 of each line based on the IP data shown in b. Results of 2 independent plants per each line are shown in triangles and circles: Red, cv. Dongjin; purple, 02764-HM; grey, 02764-WT. Note that results from Dongjin in b-d are the same data sets as those shown in b-d of Figure 3 since those experiments were performed simultaneously. The Student's-t test was performed vs. WT (a) and Dongjin (c, d), respectively: * $P < 0.05$, ** $P < 0.01$.

Figure 9. Phenotypic analyses of 02764-HM and 02764-WT plants in the vegetative growth stage under salt stress. Both genotypes were grown by hydroponic culture. Salt stress was initiated with 40 mM and 80 mM NaCl on approximately 2-week-old plants and it lasted for 21 days (a). At the end of stress treatment, (b) dry weights and (c) number of tillers per plant were measured: 02764-WT (white bars) and 02764-HM (black bars). Data represent means ±SE (n=18). Different alphabets represent significant differences (the Tukey's test).

Figure 10. Distinctive features of $^{22}Na^{+}$ allocation in two independent *OsHKT1;5* mutants. (a) $^{22}Na^{+}$ imaging analysis by direct $^{22}Na^{+}$ introduction into the cut end of leaf sheaths. 4-week-old rice seedlings treated with 10 mM NaCl for 2 days were cut at the position of 5 mm above the

root, and the cut end of the leaf sheath were placed in the solution containing 3700 Bq/ml of $^{22}Na^{+}$ for 30 min. The allocation of $^{22}Na^{+}$ in leaves 6 and 7 (L6 and L7) was analyzed using an imaging plate (IP) and line profiles of $^{22}Na^{+}$ along the sheath of L6 are presented. (b) Blade/sheath $^{22}Na^{+}$ distribution ratios of L6 and L7 (n=6, ±SD). The Student's-t test was performed vs. Dongjin: * $P < 0.05$, ** $P < 0.01$. (c) Allocation of $^{22}Na^{+}$ in young leaves (L7-9) of 4-week-old rice plants after 3 hours of the tracer uptake in roots. Rice plants treated with 10 mM NaCl for 2 days were placed into a nutrient solution containing $^{22}Na^{+}$ (1100 Bq/ml) for 3 hours, and then the radioactivity in leaf samples were measured by gamma-counter to determine the amount of Na^{+} transported to tissues of young leaves (n=3, ±SD). Note that L9 was the immature youngest leaf which was in the middle of the leaf development. Different alphabets represent significant differences (the Tukey's test).

Figure 11. A possible working model of OsHKT1;5 in Na^{+} exclusion in the vasculature of rice during salt stress, based on the present study. Schematic illustration of a longitudinal section of a rice seedling. OsHKT1;5 mediates removal of Na^{+} in the plasma membrane of the xylem parenchyma cell (XPC) in roots and sheaths, and the phloem parenchyma cell (PPC) in the DVB of basal nodes. Black lines in the seedling represent vascular bundles and a wider part in the basal stem shows an enlarged vascular region that includes DVBs. Note that sieve tubes that locates in this enlarged region lacks phloem companion cells and thus the tubes are surrounded by PPCs.

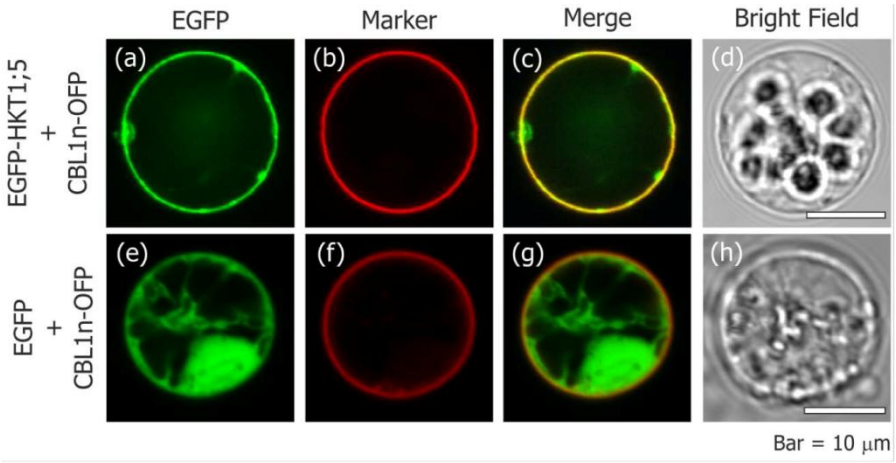

(a)

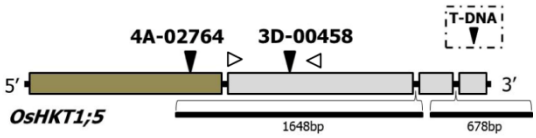

(b)

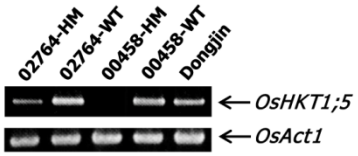

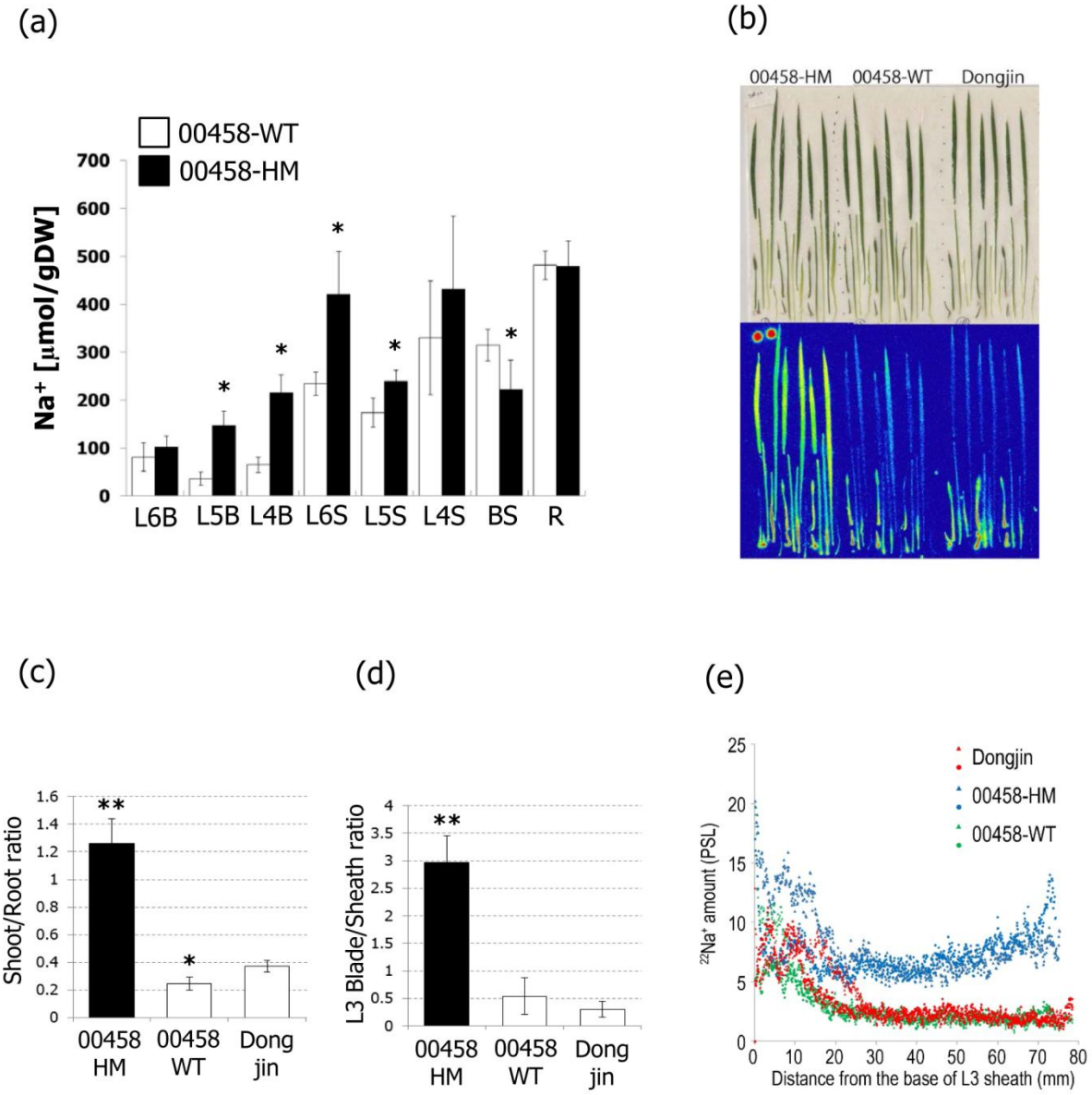

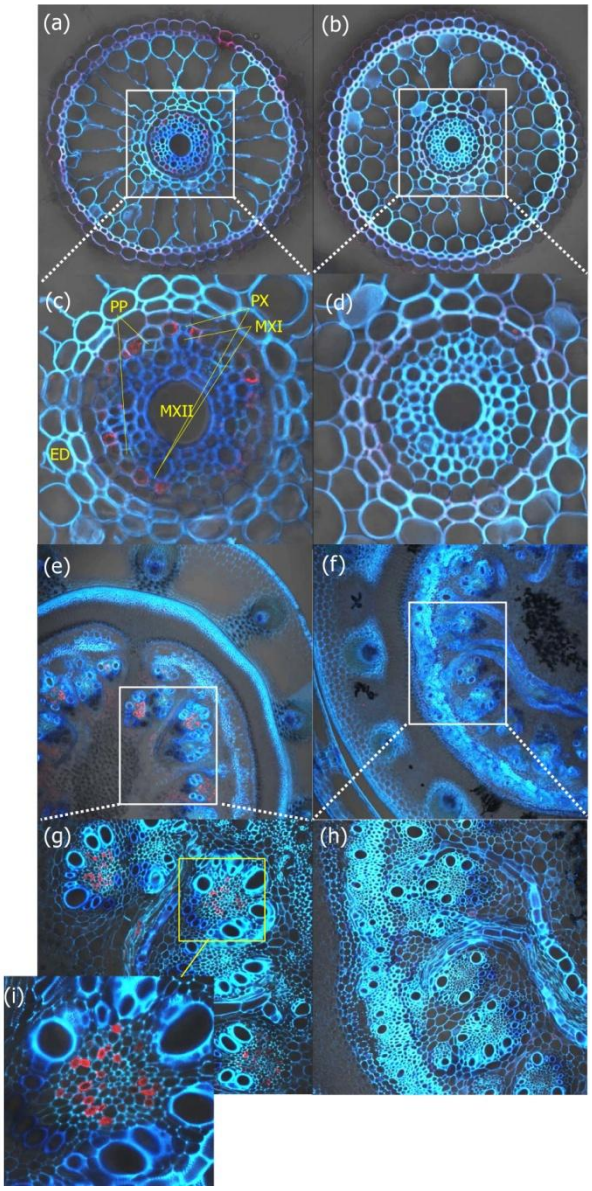

(a)

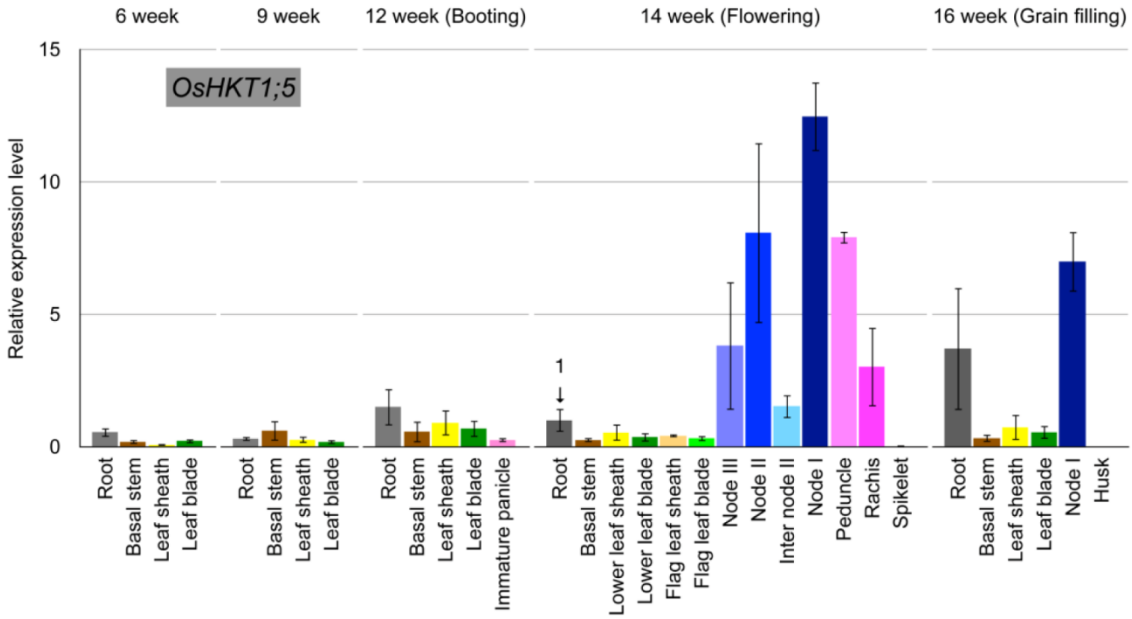

(b)